Influence of the Incorporation of Fine Calcium Carbonate Particles on the Impact Strength of Polypropylene/Polystyrene-*block*-Poly(ethylene butene)-*block*-Polystyrene Blends

Shigeki Hikasa,[1] Kazuya Nagata,[2] Kenji Miyahara,[3] Toshihiro Izumi,[3] Toshiya Suda,[3] Asami Toyohara,[3] Atushi Kato,[3] Yoshinobu Nakamura[4]

[1]Industrial Technology Center of Okayama Prefecture Government, 5301 Haga, Okayama 701-1296, Japan
[2]Advanced Technology Development Department, Laboratory of Plastics, Asahi Kasei Chemicals Corporation, 1-3-1 Yacoh, Kawasaki-Ku, Kawasaki, Kanagawa, 210-0863 Japan
[3]Material Research Center, Research Department, Nissan ARC, Limited, 1 Natsushima-Cho, Yokosuka, Kanagawa, 237-0061 Japan
[4]Department of Applied Chemistry, Osaka Institute of Technology, 5-16-1 Ohmiya, Asahi-Ku, Osaka 535-8585, Japan

ABSTRACT: The Izod impact strength of two kinds of ternary composites was investigated. One consisted of polypropylene (PP), the triblock copolymer polystyrene-*block*-poly(ethylene butene)-*block*-polystyrene (SEBS), and calcium carbonate ($CaCO_3$) particles, and the other consisted of PP, carboxylated SEBS (C-SEBS), and $CaCO_3$ particles. The mean size of the $CaCO_3$ particles was about 160 nm. According to scanning electron microscopy observations, the composite with SEBS showed a morphology in which SEBS domains and $CaCO_3$ particles were independently dispersed in the PP matrix. On the other hand, the composite with C-SEBS showed a morphology in which $CaCO_3$ particles were encapsulated by C-SEBS; that is, a core–shell structure was formed. The Izod impact strength of the composite with SEBS was higher than that of the composite with C-SEBS and the PP/SEBS and PP/C-SEBS binary blends. According to observations of the fractured surface, the stress-whitened area was larger in the composite with SEBS than in the composite with C-SEBS and the PP/SEBS and PP/C-SEBS binary blends. The toughening mechanism of the composite, using nanometer-sized $CaCO_3$ particles in combination with SEBS, was examined. © 2009 Wiley Periodicals, Inc. J Appl Polym Sci 114: 919–927, 2009

Key words: composites; elastomers; impact resistance; morphology; poly(propylene) (PP)

INTRODUCTION

Particle-filled polypropylene (PP) composites are widely used in various industrial fields (e.g., plastic parts for automobiles). The addition of fillers such as talc and glass fibers improves some mechanical properties of PP, namely the modulus and heat distortion temperature. However, the addition of fillers decreases the impact strength of PP composites. On the other hand, elastomer modification improves the impact strength of PP composites at the expense of the modulus. Therefore, ternary composites consisting of PP, an elastomer, and a filler are becoming attractive materials because they possess both a high modulus and a high impact strength.

It has been explained that the mechanical properties of such ternary composites are strongly influenced by both the composition and the morphology.[1,2] The morphology is strongly dependent on both the interfacial interaction between the components and the mixing method.[1–3]

Two different morphologies are expected to form in PP/elastomer/filler ternary composites. One is a morphology with the elastomer and filler particles dispersed independently in the PP matrix. Another has core–shell-type particles consisting of a filler particle core and an elastomer shell. The formation of these morphologies is reported to be strongly dependent on the interactions of the elastomer and filler.[1–3] When no functional group is introduced into the elastomer, the elastomer and the filler particles are dispersed independently in the PP matrix because there is no interaction between the elastomer and the filler particles. On the other hand, when the functionalized elastomer is used to enhance the interaction between the elastomer and filler, the aforementioned core–shell structure should be formed. The morphology is also affected by the mixing methods used for the composite preparation. Nakata et al.[4] reported that a core–shell morphology was promoted by a two-step mixing process. That is,

an elastomer/filler mixture was prepared as a master batch in the first step, and then the prepared master batch was mixed with PP in the second step. As a result, a core–shell structure was formed. However, a morphology in which the elastomer and filler particles were dispersed independently was formed with a one-step mixing process.

These PP/elastomer/filler ternary composites with a core–shell morphology have been reported to have a slightly higher impact strength and lower modulus than those with an independently dispersed morphology for the following reasons.[1–4] First, the apparent elastomer volume fraction in the core–shell morphology is larger than that in the independently dispersed morphology because the elastomer particles are involved with the filler. Second, when an impact load is applied to a ternary composite, the crack initiated from the edge of the filler propagates in the PP matrix. The elastomer encapsulating the filler inhibits crack initiation from the edge or terminates the propagating crack in the PP matrix.[1,5,6]

As mentioned previously, there are many reports about the relation between the morphology and impact properties of PP/elastomer/filler ternary composites with filler particles with a mean size above 1 μm. Recently, we reported that the incorporation of calcium carbonate ($CaCO_3$) particles with a mean size below 1 μm improved the impact strength of a PP/$CaCO_3$ binary composite,[7] a poly(vinyl chloride)/chlorinated polyethylene/$CaCO_3$ ternary composite,[8] and a poly(vinyl chloride)/methyl methacrylate–butadiene–styrene copolymer/$CaCO_3$ ternary composite.[9] Nomura[10] also explained that $CaCO_3$ fine particles with a mean size of about 150 nm improved the impact strength of a PP/ethylene–propylene rubber/$CaCO_3$ ternary composite. However, the effect of the morphology was hardly discussed in these previous studies.

In this study, therefore, the influence of the morphology on the mechanical properties of PP/elastomer/filler ternary composites was studied with the triblock copolymer polystyrene-*block*-poly(ethylene butene)-*block*-polystyrene (SEBS) or carboxylated SEBS (C-SEBS) as the elastomer and with fine $CaCO_3$ particles having a mean diameter of about 160 nm as the filler. Such nanometer-sized $CaCO_3$ particles have a far larger particle number than common micrometer-sized particles. The particles in a composite act as stress-concentrated points, and the concentrated stress forms microdeformation, such as shear yielding around the particles. The effect is expected to increase with an increase in the particle number. Morphologies with an independently dispersed structure and with a core–shell structure were formed with SEBS and C-SEBS, respectively. The morphology was observed with scanning electron microscopy (SEM). As a result, a far larger

improvement in the impact strength with the addition of fine filler particles, in comparison with those reported previously, was obtained.

EXPERIMENTAL

Materials

The PP used as a matrix in this study was homo-PP (melt index = 8; PM600A, SunAllomer, Ltd., Tokyo, Japan). The elastomers used were SEBS (trial production, D-14, Asahi Kasei Chemicals Corp., Tokyo, Japan) and C-SEBS (trial production, C-12, Asahi Kasei Chemicals). The $CaCO_3$ particles were synthesized $CaCO_3$ (Calseeds P, Konoshima Chemical Co., Ltd., Osaka, Japan) with a mean diameter of about 160 nm and a specific surface area of 8 m^2/g. The surface was treated with a fatty acid to prevent the aggregation of $CaCO_3$ particles.

Sample preparation

PP, an elastomer (SEBS or C-SEBS), and $CaCO_3$ were compounded with a TEX-30α corotating twin-screw extruder (length/diameter ratio = 42, screw diameter = 30 mm) from Japan Steel Works, Ltd. (Tokyo, Japan), with a one-step procedure. The extrusion temperatures were set from 160 to 210°C at the different zones from the hopper to the die. The screw speed was 100 rpm.

The test specimens for mechanical properties, about 3 mm thick, were prepared by injection molding (J50EII, Japan Steel Works). The injection temperatures from the hopper to the nozzle were 190, 210, 220, and 230°C, and the mold temperature was 45°C. Before injection molding, the granules of the composites were dried in an oven at 80°C for 4 h.

Characterization of the composites

The fractured surfaces of the composites in liquid N_2 were stained by RuO_4 vapor at 25°C for 1 h. The surfaces were observed by SEM (Hitachi S-4700, Hitachi High-Technologies Corp., Tokyo, Japan) to examine the morphology. The fractured surfaces were coated with Pt and observed with SEM.

Calculation of the average size of the SEBS particles

The fractured specimens were immersed in toluene at 20°C for 10 min to remove SEBS particles from the PP matrix. SEM observation showed that many holes were formed in the surfaces of the specimens immersed in toluene. The apparent average size of the SEBS particles was measured via image analysis (Image-Pro Plus, version 4, Media Cybernetics, Inc., Bethesda, MD) with the SEM image of the surface.
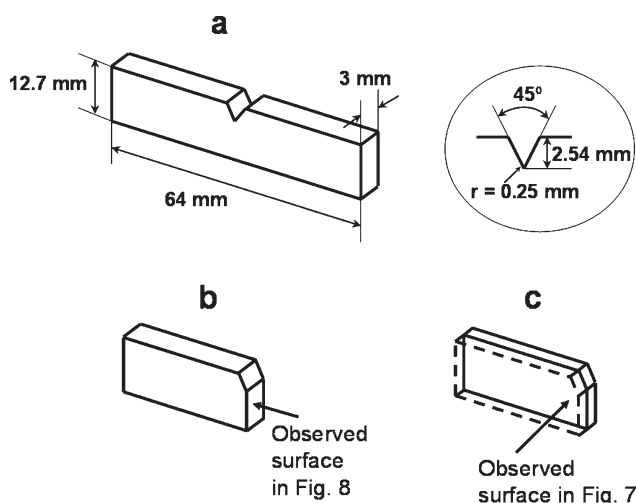
Figure 1 Shape and size of (a) the original Izod impact test specimen, (b) the fractured specimen after the test, and (c) the vertically half-cut, fractured specimen after the test.

Flexural properties

Flexural properties were measured at 23°C and a relative humidity of 50% with a tensile testing machine (type 5583, Instron Japan Co., Ltd., Kanagawa, Japan). Flexural testing was carried out with plate-shaped specimens (JIS K7171, which corresponds to ISO 178) at a crosshead rate of 2 mm/min. The thickness of the specimens was 3 mm.

Impact properties

The Izod impact strength was measured with a notched specimen and an impact tester (type 258-D, Yasuda Seiki Seisakusyo, Ltd., Hyogo, Japan) in accordance with JIS K7110 (which corresponds to ISO 180). The shape and size of the Izod test specimen are shown in Figure 1(a). A V-shaped notch with a tip radius of 0.25 mm was machined (JIS type 2A). The test was performed at 23°C and a relative humidity of 50%.

Fracture analysis

The parts of the fractured Izod impact test specimen observed with an optical microscope (Coolpix 950, Nikon Corp., Tokyo, Japan) are shown in Figure 1(b,c). A vertical view of the fractured notch front region is also shown [Fig. 1(c)]. The part shown as a broken line was cut, and the surface was polished with sandpapers (from 120 to 1200), which were followed by alumina and diamond powders in flowing water, with an autopolishing machine (ATU338, Refinetec Corp., Kanagawa, Japan).

RESULTS AND DISCUSSION

Morphology

Figure 2 shows SEM images of the PP/SEBS (80/20 v/v) binary blend. The specimen was cut with a low-temperature microtome after being frozen in liquid N_2, and the obtained surface was observed by SEM after staining with RuO_4. Figure 2(a,b) shows backscattered electron and secondary electron images, respectively, for the same field of view. RuO_4 stains polystyrene parts in SEBS preferentially. Therefore, the white areas with diameters in the range of 200–600 nm show the SEBS elastomer particles in the backscattered electron image [Fig. 2(a)]. To confirm this point, the fractured surface was immersed in toluene, and the SEBS elastomer particles were extracted. Toluene is a good solvent for SEBS but not for PP.

Figure 3 shows the SEM image of the fractured surface from which elastomer domains were extracted. The composition was 85/15 (v/v) PP/SEBS. Many holes could be clearly observed. From this result, it was confirmed that the white areas in Figure 2(a) show the SEBS elastomer particles. In Figure 2(a,b), the backscattered electron image and the secondary electron image are similar. Therefore, the SEM observation was performed with the secondary electron image only.
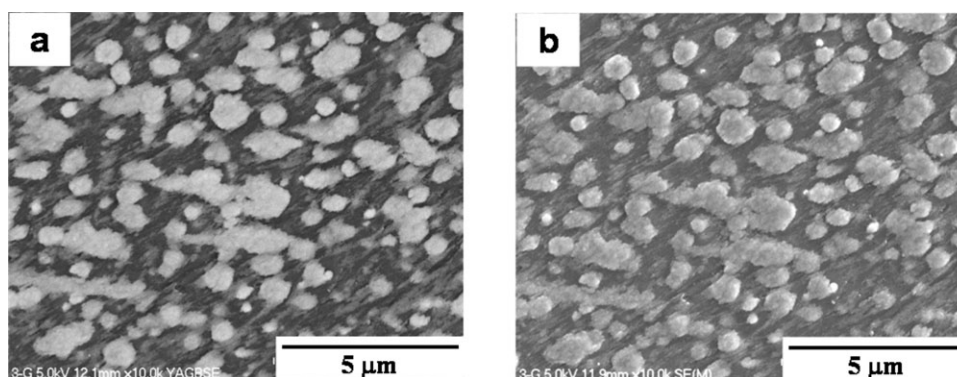

Figure 2 Cut surfaces of the PP/SEBS (80/20 v/v) binary blend for (a) backscattered electron and (b) secondary electron images observed by SEM. The specimen was cut with a low-temperature microtome after being frozen in liquid N_2.
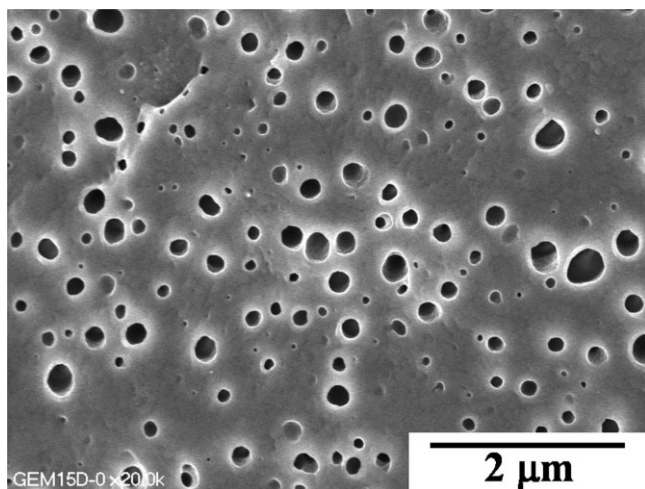
Figure 3 Fractured surface of the PP/SEBS (85/15 v/v) binary blend observed by SEM. The specimen was fractured in liquid N_2. Elastomer domains were extracted by immersion in toluene.

Figure 4 shows the SEM images (secondary electron images) of PP/SEBS and PP/C-SEBS binary blends and PP/SEBS/CaCO$_3$ and PP/C-SEBS/CaCO$_3$ ternary composites. The specimens were fractured in liquid N_2, and the surface was observed by SEM after staining with RuO$_4$. In the PP/SEBS binary blend [Fig. 4(a)], the whiter areas with diameters in the range of 50–600 nm show the SEBS elastomer particles. In the PP/C-SEBS binary blend [Fig. 4(b)], the diameter was in the range of 40–1200 nm. The elastomer particles were larger in the PP/C-SEBS blend than in the PP/SEBS binary blend because the compatibility of PP and C-SEBS was lower than that of PP and SEBS.

In the PP/SEBS/CaCO$_3$ ternary composite [Fig. 4(c)], the spherical SEBS elastomer particles with diameters in the range of 80–330 nm and the irregularly shaped CaCO$_3$ particles with a mean diameter of about 160 nm were observed independently in the PP matrix. Both the single particle and the agglomerates of several CaCO$_3$ particles were observed.

In the PP/C-SEBS/CaCO$_3$ ternary composite [Fig. 4(d)], the independent C-SEBS elastomer particles and CaCO$_3$ particles were rarely observed. The agglomerated CaCO$_3$ particles were present in the C-SEBS elastomer particles; that is, they formed the core–shell structure. The size of the agglomerated CaCO$_3$ particles was larger in the PP/C-SEBS/CaCO$_3$ ternary composite [Fig. 4(d)] than in the PP/SEBS/CaCO$_3$ ternary composite [Fig. 4(c)].

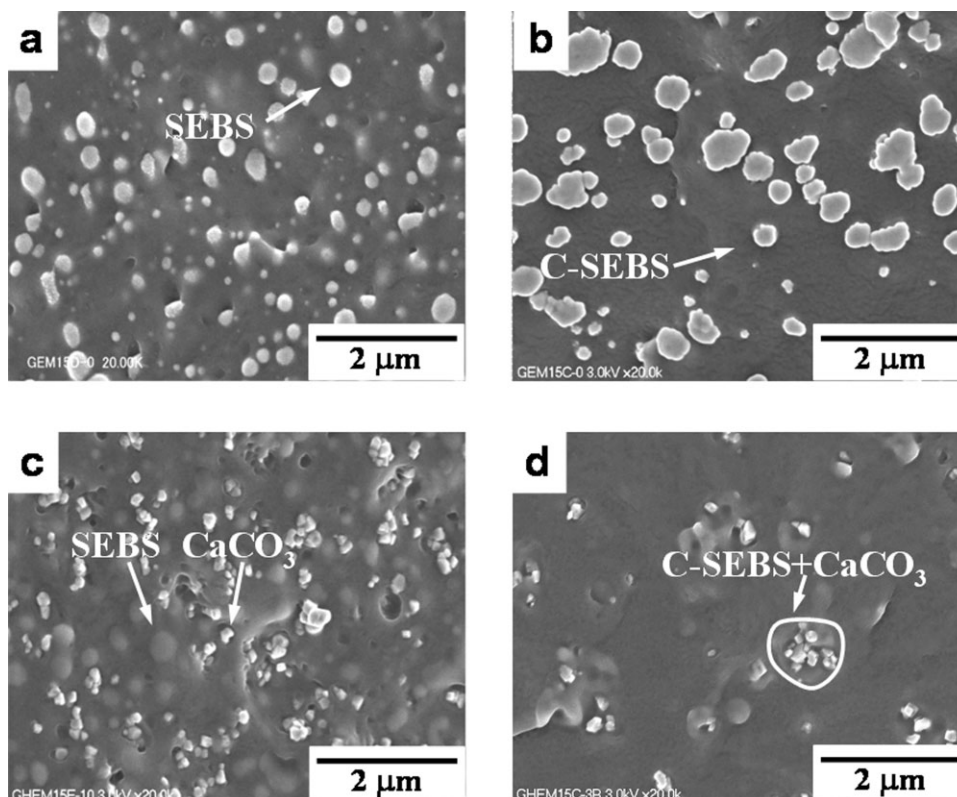These morphologies were dependent on the existence of the carboxyl group in SEBS, that is, the

Figure 4 Fractured surfaces of (a) the PP/SEBS (85/15 v/v) binary blend, (b) the PP/C-SEBS (85/15 v/v) binary blend, (c) the PP/SEBS/CaCO$_3$ (82/15/3 v/v) ternary composite, and (d) the PP/C-SEBS/CaCO$_3$ (82/15/3 v/v) ternary composite observed by SEM. The specimens were fractured in liquid N_2.
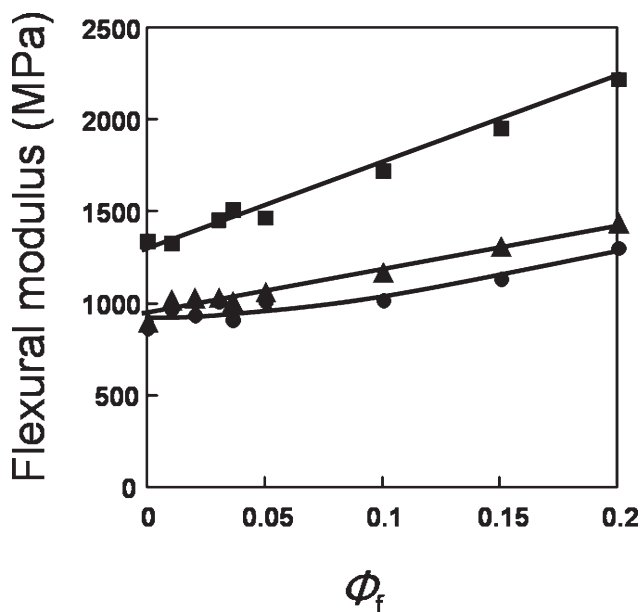
Figure 5 Relation between the flexural modulus and ϕ_f (■) without an elastomer, (▲) with SEBS, and (●) with C-SEBS. ϕ_e was 0.20.

difference in the interactions of SEBS/CaCO$_3$ and C-SEBS/CaCO$_3$. It was reported that CaCO$_3$ particles were encapsulated with a carboxylated polymer because of the ionic interaction between the CaCO$_3$ surface and carboxyl group when the carboxylated polymer was used in a composite.[7] For the same reason, the CaCO$_3$ particles were encapsulated by C-SEBS in the PP/C-SEBS/CaCO$_3$ ternary composite in this study. However, the SEBS and CaCO$_3$ particles were dispersed independently in the PP/SEBS/CaCO$_3$ ternary composite because there was no ionic interaction between SEBS and CaCO$_3$.

Modulus

Figure 5 shows the relation between the flexural modulus of the ternary composites and the volume fraction of filler CaCO$_3$ particles (ϕ_f). The volume fraction of the elastomer (SEBS or C-SEBS) in the composite (ϕ_e) was 0.20. The flexural modulus of the PP/CaCO$_3$ binary composites was higher than that of the PP/elastomer/CaCO$_3$ ternary composites. The incorporation of the elastomer lowered the modulus. The flexural moduli of the PP/CaCO$_3$ binary composite and the PP/SEBS/CaCO$_3$ and PP/C-SEBS/CaCO$_3$ ternary composites increased with an increase in ϕ_f. However, the flexural modulus of the PP/C-SEBS/CaCO$_3$ ternary composite was lower than that of the PP/SEBS/CaCO$_3$ ternary composite, although their ϕ_f values were the same.

These results were caused by the differences in their morphologies. The encapsulating soft elastomer layer on the CaCO$_3$ particle surface reduced the reinforcement effect by the CaCO$_3$ filler particles in the PP/C-SEBS/CaCO$_3$ ternary composite.[1,2]

Impact strength

Figure 6 shows the relation between the notched Izod impact strength and ϕ_e for the PP/SEBS/CaCO$_3$ and PP/C-SEBS/CaCO$_3$ ternary composites, respectively. The impact strength improved drastically with the incorporation of SEBS beyond $\phi_e \approx 0.2$ in the PP/SEBS binary blend [$\phi_f = 0$; solid line, Fig. 6(a)]. A similar result was obtained for the PP/C-SEBS binary blend [$\phi_f = 0$; solid line, Fig. 6(b)].

Further improvement of the impact strength was obtained with the addition of CaCO$_3$ particles. The remarkably improved impact strength values with
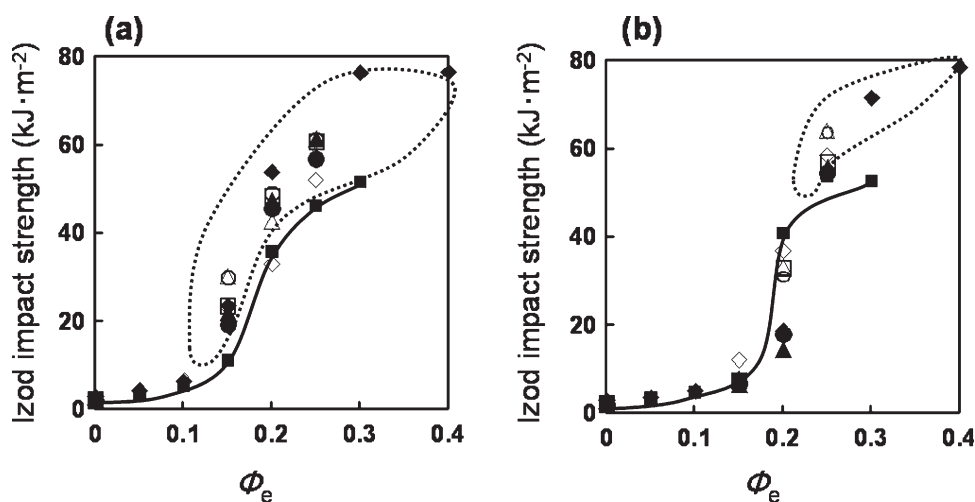

Figure 6 Relation between the Izod impact strength and ϕ_e for (a) PP/SEBS/CaCO$_3$ and (b) PP/C-SEBS/CaCO$_3$ ternary composites with various ϕ_f values: (■) 0, (●) 0.01, (▲) 0.03, (◆) 0.04, (□) 0.05, (○) 0.10, (△) 0.15, and (◇) 0.20. The points at which the synergistic effect with the addition of the filler and elastomer appeared are enclosed by the dotted line. The solid line indicates the results without the filler.
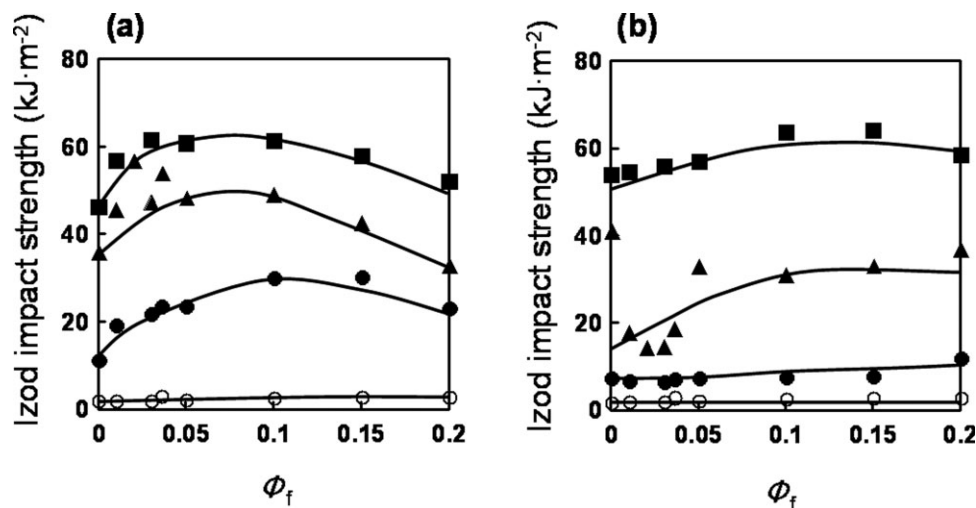
Figure 7 Relation between the Izod impact strength and ϕ_f for (a) PP/SEBS/CaCO$_3$ and (b) PP/C-SEBS/CaCO$_3$ ternary composites with various ϕ_e values: (○) 0, (●) 0.15, (▲) 0.20, and (■) 0.25.

the addition of CaCO$_3$ particles are surrounded by the dotted loops in Figure 6. The impact strength was improved in the wider ϕ_f and ϕ_e ranges in the PP/SEBS/CaCO$_3$ ternary composite [Fig. 6(a)] versus the PP/C-SEBS/CaCO$_3$ ternary composite [Fig. 6(b)]. That is, the higher improvement effect of the impact strength was obtained in the morphology in which the filler and elastomer particles were dispersed independently rather than in the morphology having a core–shell structure in this study. This result was the opposite of that reported previously.[1,2,4]

Figure 7 shows the relation between the notched Izod impact strength and ϕ_f for the PP/SEBS/CaCO$_3$ and PP/C-SEBS/CaCO$_3$ ternary composites. ϕ_e was in the range of 0.15–0.25. The improvement effect of the impact strength was higher in the PP/SEBS/CaCO$_3$ ternary composite [Fig. 7(a)] than in the PP/C-SEBS/CaCO$_3$ ternary composite [Fig. 7(b)] for the ϕ_e values of 0.15, 0.20, and 0.25. In the PP/SEBS/CaCO$_3$ ternary composite, the impact strength increased with an increase in ϕ_f and reached the maximum value, and the values decreased gradually with ϕ_f [Fig. 7(a)]. In the PP/C-SEBS/CaCO$_3$ ternary composite, the impact strength increased with ϕ_f more gradually than in the PP/SEBS/CaCO$_3$ ternary composite. That reached a constant value [Fig. 7(b)]. In the ϕ_e range of 0.15–0.25, the degree of increase in the impact strength with ϕ_f was larger in the PP/SEBS/CaCO$_3$ ternary composite [Fig. 7(a)] than in the PP/C-SEBS/CaCO$_3$ ternary composite [Fig. 7(b)] below the ϕ_f value of 0.1 and ϕ_e values of 0.15–0.20.

Many researchers have reported that elastomer blending improves the impact strength of PP.[4,11,12] A similar result was obtained in this study: the impact strength of the PP/SEBS blend was improved significantly above $\phi_e = 0.15$, as shown in Figure 6. It has

also been reported that the incorporation of filler particles decreases the impact strength of PP/elastomer/filler ternary composites. In addition, a higher impact strength has also been reported for the morphology in which the elastomer and filler particles form a core–shell structure versus the morphology in which the elastomer and the filler particles are independently dispersed with the same ϕ_e and ϕ_f values.[1–4,13]

The explained first reason for this result is that the encapsulated filler with the elastomer acted as a true elastomer particle, so the apparent elastomer content increased in the morphology with a core–shell structure. Other reasons are also explained as follows.

Li et al.[2] clarified that the elastomer shell of the core–shell structure is stretched between the filler particle surface and PP matrix and that the elastomer forms filaments when the impact stress is applied. Then, the formed filaments of the elastomer contribute to the formation of the shear yielding ribbon in the PP matrix. Long et al.[1] observed that the crack initiated from the filler particle is terminated by the elastomer particle, resulting in the formation of the shear yielding ribbon.

However, the higher impact strength was obtained by the addition of CaCO$_3$ particles with a mean size of about 160 nm to the PP/SEBS/CaCO$_3$ ternary composite rather than to the PP/SEBS binary blend in this study (Fig. 6). The filler and elastomer particles were dispersed independently in the PP/SEBS/CaCO$_3$ ternary composite. The impact strength increased with the addition of CaCO$_3$ particles below $\phi_f = 0.1$ in the PP/SEBS/CaCO$_3$ ternary composite [Fig. 7(a)]. The degree of the increase in the impact strength with ϕ_f was larger in the PP/SEBS/CaCO$_3$ ternary composite than in the PP/C-SEBS/CaCO$_3$ ternary composite below $\phi_f = 0.1$. These
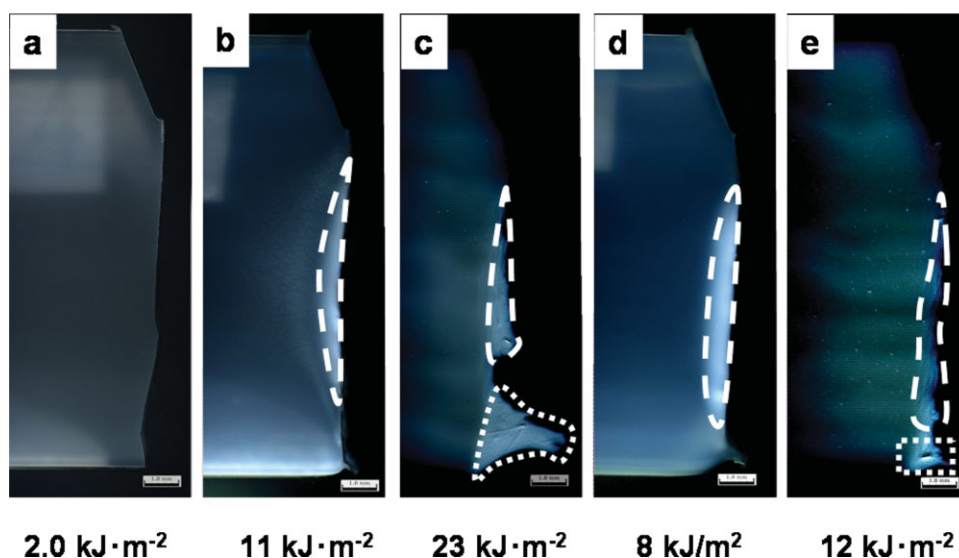
Figure 8 Polished surfaces of vertically cut, fractured Izod impact test specimens of (a) PP, (b) the PP/SEBS (80/20 v/v) binary blend, (c) the PP/SEBS/CaCO$_3$ (64/16/20 v/v) ternary composite, (d) the PP/C-SEBS (80/20 v/v) binary blend, and (e) the PP/C-SEBS/CaCO$_3$ (64/16/20 v/v) ternary composite observed with an optical microscope. The stress-whitened area is enclosed by the broken line, and the unbroken area is enclosed by the dotted line. The Izod impact strength value is shown beneath each photograph. [Color figure can be viewed in the online issue, which is available at www.interscience.wiley.com.]

results obtained in this study were quite different from those reported previously in which the filler particles had a diameter greater than 1 μm.[1–4]

Next, an analysis of the fracture phenomenon was carried out to clarify the improvement mechanism for the impact strength by the synergy effect, with both the elastomer and the fine filler particles having a diameter of about 160 nm.

Figure 8 shows the cross sections of fractured notched Izod impact specimens of PP, the PP/SEBS binary blend, the PP/SEBS/CaCO$_3$ ternary composite, the PP/C-SEBS binary blend, and the PP/C-SEBS/CaCO$_3$ ternary composite observed with an optical microscope. The areas enclosed by a broken line are the stress-whitened areas. These specimens were cut to half of the thickness, and the surfaces were polished before observation. PP showed a typical brittle fracture [Fig. 8(a)]. There was no stress-whitened area. On the other hand, the stress-whitened areas were clearly observed in the binary blends [Fig. 8(b,d)] and the ternary composites [Fig. 8(c,e)]. In the PP/SEBS/CaCO$_3$ ternary composite [Fig. 8(c)], the crack propagated with the impact stress, but the specimen was never fractured completely, and the unbroken part of the specimen was elongated by the hammer of the Izod impact tester. The elongated part in the fractured specimen is enclosed by the dotted line in Figure 8(c), and the area is called the unbroken area. That is, it was never completely broken by the impact, and this means that the PP/SEBS/CaCO$_3$ ternary composite was most ductile.

In the PP/C-SEBS/CaCO$_3$ ternary composite [Fig. 8(e)], a similar fracture phenomenon was observed, whereas the unbroken area was far smaller than that of the PP/SEBS/CaCO$_3$ ternary composite [Fig. 8(c)]. The stress-whitened area contained an unbroken area that was larger in the PP/SEBS/CaCO$_3$ ternary composite [Fig. 8(c)] than in the PP/C-SEBS/CaCO$_3$ ternary composite [Fig. 8(e)]. The area was larger in the PP/SEBS/CaCO$_3$ [Fig. 8(c)] and PP/C-SEBS/CaCO$_3$ ternary composites [Fig. 8(e)] than in the PP/SEBS [Fig. 8(b)] and PP/C-SEBS binary blends [Fig. 8(d)].

The Izod impact strength values are shown below each optical micrograph. There was a good relation between the stress-whitened area and the Izod impact strength value.

Figure 9 shows the fractured surfaces of notched Izod impact specimens of PP, the PP/SEBS binary blend, the PP/SEBS/CaCO$_3$ ternary composite, the PP/C-SEBS binary blend, and the PP/C-SEBS/CaCO$_3$ ternary composite observed with an optical microscope. The fractured surface of PP [Fig. 9(a)] was a plane, and this indicated brittle fracture. The surface was rougher in the PP/SEBS [Fig. 9(b)] and PP/C-SEBS binary blends [Fig. 9(d)]. Furthermore, a far rougher surface was observed in the PP/SEBS/CaCO$_3$ [Fig. 9(c)] and PP/C-SEBS/CaCO$_3$ ternary composites [Fig. 9(e)]. The unbroken area was larger in the PP/SEBS/CaCO$_3$ ternary composite [Fig. 9(c)] than in the C-SEBS/CaCO$_3$ ternary composite [Fig. 9(e)]. According to the observation of the fractured surface, the ductile property was higher in the
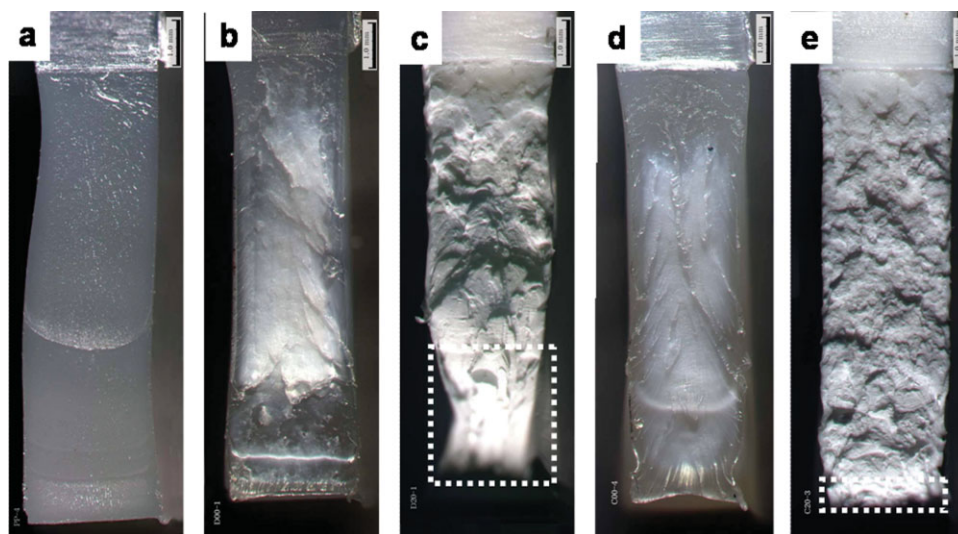
Figure 9 Fractured surfaces of Izod impact test specimens of (a) PP, (b) the PP/SEBS (80/20 v/v) binary blend, (c) the PP/SEBS/CaCO$_3$ (64/16/20 v/v) ternary composite, (d) the PP/C-SEBS (80/20 v/v) binary blend, and (e) the PP/C-SEBS/CaCO$_3$ (64/16/20 v/v) ternary composite observed with an optical microscope. The unbroken area is enclosed by the dotted line. [Color figure can be viewed in the online issue, which is available at www.interscience.wiley.com.]

following order: PP/SEBS/CaCO$_3$ ternary composite > C-SEBS/CaCO$_3$ ternary composite > PP/SEBS binary blend = PP/C-SEBS binary blend.

Suzuki and Ishikawa[14] reported that well-dispersed fine CaCO$_3$ particles with a mean diameter of about 1 μm improved the impact strength of PP by the following mechanism. The debonding of the PP matrix and CaCO$_3$ particles occurred and voids were formed when the impact load was applied. As a result, the concentrated strain around the CaCO$_3$ particles was reduced. Narisawa et al.[11,12] clarified that shear yielding ribbons formed, followed by debonding; as a result, an extreme improvement of the impact strength was obtained.[11,12] From these studies, crack propagation seemed to be blocked by the formation of a damage zone, such as debonding, void formation, and shear yielding.

In Figure 8, the largest stress-whitened area can be observed for the PP/SEBS/CaCO$_3$ ternary composite. The stress-whitened area is thought to be the damage zone consisting of debonding of the particle/matrix interface, voids and crazing, and shear yielding ribbons around the filler or elastomer particles. The stress-whitened area was expected to reduce the applied strain and to block crack propagation. Therefore, the impact strength was dependent on the size of the stress-whitened area, as shown in Figure 8. The morphology in which the SEBS elastomer particles and the fine CaCO$_3$ particles were dispersed independently seemed to form the damage zone most effectively.

The estimated mechanism is shown next. When the impact stress was applied, debonding of the elastomer particle/matrix interface or void formation (cavitation) of the elastomer particles occurred in the PP/SEBS/CaCO$_3$ ternary composite. The void formation generated shear yielding ribbons around the elastomer particles. Growth of the shear yielding ribbons was depressed by the fine CaCO$_3$ particles dispersed in the PP matrix. As a result, many small shear yielding ribbons were formed in the PP matrix, and then they improved the impact strength.

On the other hand, in the PP/C-SEBS/CaCO$_3$ ternary composite, the CaCO$_3$ particles were encapsulated by C-SEBS and never dispersed independently in the PP matrix. Therefore, the CaCO$_3$ particles hardly depressed the growth of the shear yielding ribbon. This is the reason that the impact strength of the PP/C-SEBS/CaCO$_3$ ternary composite was lower than that of the PP/SEBS/CaCO$_3$ ternary composite.

CONCLUSIONS

The effect of the addition of fine CaCO$_3$ particles to PP/SEBS and PP/C-SEBS blends on the impact strength was investigated. The following results were obtained:

1. According to SEM observations, the PP/SEBS/CaCO$_3$ ternary composite showed the morphology in which the SEBS domains and CaCO$_3$ particles were independently dispersed in the PP matrix. On the other hand, the PP/C-SEBS/CaCO$_3$ ternary composite showed the morphology in which CaCO$_3$ particles were encapsulated by C-SEBS; that is, a core–shell structure was formed.

2. The impact strength was improved most effectively in the PP/SEBS/CaCO$_3$ ternary composite.
3. According to the observation of the fractured surface, the stress-whitened area was largest in the PP/SEBS/CaCO$_3$ ternary composite. There was a good relation between the stress-whitened area and the Izod impact strength.
4. PP showed typical brittle fracture, whereas the PP/SEBS/CaCO$_3$ ternary composites showed ductile fracture. It was concluded that the morphology in which the SEBS elastomer particles and the fine CaCO$_3$ particles were dispersed independently most effectively influenced the formation of the damage zone.

References

1. Long, Y.; Shanks, R. A. J Appl Polym Sci 1996, 61, 1877.
2. Li, Z.; Go, S.; Song, W.; Hou, B. J Mater Sci 2003, 38, 1793.
3. Long, Y.; Shanks, R. A. J Appl Polym Sci 1996, 62, 639.
4. Nakata, H.; Higashida, N.; Takamatsu, H. J Jpn Soc Polym Process 2000, 12, 781.
5. Nagata, K.; Hikasa, S.; Nishi, K.; Iwabuki, H. J Soc Rubber Ind Jpn 2006, 79, 267.
6. Long, Y.; Shanks, R. A. Annu Tech Conf 1996, 96, 3673.
7. Nagata, K.; Nigo, H.; Hikasa, S.; Ito, R. J Adhes Soc Jpn 2002, 38, 2.
8. Nagata, K.; Fujiwara, K.; Hikasa, S.; Nigo, H.; Ito, R. J Adhes Soc Jpn 2003, 39, 4.
9. Nagata, K.; Fujiwara, K.; Hikasa, S.; Nigo, H.; Ito, R. J Adhes Soc Jpn 2003, 39, 169.
10. Nomura, M. Plastics 1995, 46, 45.
11. Takaki, A.; Yamazaki, K.; Narisawa, I. Polym Eng Sci 2000, 40, 398.
12. Takaki, A.; Yamazaki, K.; Narisawa, I. Polym Eng Sci 2001, 41, 575.
13. Hikasa, S.; Nagata, K.; Maekawa, K.; Yoshihara, M.; Komiya, Y. Kobunshi Ronbunsyu 2004, 61, 573.
14. Suzuki, H.; Ishikawa, M. Proc Jpn Soc Polym Proc Symp 2005, 13, 79.